

Next-to-leading-order QCD corrections to $e^+e^- \rightarrow H + \gamma$

Wen-Long Sang ¹

School of Physical Science and Technology, Southwest University, Chongqing 400700, China

Wen Chen ²

Institute of High Energy Physics and Theoretical Physics Center for Science Facilities, Chinese Academy of Sciences, Beijing 100049, China

School of Physics, University of Chinese Academy of Sciences, Beijing 100049, China

Feng Feng ³

China University of Mining and Technology, Beijing 100083, China

Institute of High Energy Physics and Theoretical Physics Center for Science Facilities, Chinese Academy of Sciences, Beijing 100049, China

Yu Jia ⁴

Institute of High Energy Physics and Theoretical Physics Center for Science Facilities, Chinese Academy of Sciences, Beijing 100049, China

School of Physics, University of Chinese Academy of Sciences, Beijing 100049, China

Center for High Energy Physics, Peking University, Beijing 100871, China

Qing-Feng Sun ⁵

Department of Modern Physics, University of Science and Technology of China, Hefei, Anhui 230026, China

Institute of High Energy Physics and Theoretical Physics Center for Science Facilities, Chinese Academy of Sciences, Beijing 100049, China

Abstract

The associated production of Higgs boson with a hard photon in lepton collider, *i.e.*, $e^+e^- \rightarrow H\gamma$, is known to bear a rather small cross section in Standard Model, and may serve a sensitive channel to probe the potential new physics signals. Similar to the loop-induced Higgs decay processes $H \rightarrow Z/\gamma + \gamma$, this associated production process also starts at one-loop order if the exceedingly small electron Yukawa coupling is turned off. In this work, we calculate the next-to-leading-order QCD corrections to $e^+e^- \rightarrow H\gamma$, which occur at the two-loop order and stem mainly from the gluonic dressing to the top quark loop. The QCD corrections are found to be rather modest at lower center-of-mass energy range ($\sqrt{s} < 300$ GeV), thus of negligible impact on Higgs factory such as CEPC. Nevertheless, when the energy is boosted to the ILC energy range ($\sqrt{s} \approx 400$ GeV), the QCD corrections may reach 20% of the leading-order cross section.

¹wlsang@ihep.ac.cn

²chenwen@ihep.ac.cn

³F.Feng@outlook.com

⁴jiay@ihep.ac.cn

⁵qfsun@mail.ustc.edu.cn

1. Introduction

After the historical discovery of the 125 GeV boson by the ATLAS and CMS collaborations at LHC in 2012 [1, 2], a great amount of efforts have been devoted to unravelling its nature. Numerous evidences have been accumulating, to indicate that this new particle is the long-sought Higgs boson, which plays the pivotal role in initiating spontaneous electroweak symmetry breaking. To date, the measured couplings between Higgs boson and heavy fermions and gauge bosons are compatible with the Standard Model (SM) predictions within the 10% – 20% accuracy [3].

One of the central goals of contemporary high-energy physics is to precisely nail down the properties of the Higgs boson, and to search for the footprint of new physics in the Higgs sector. Due to the enormous backgrounds at hadron colliders, lepton colliders are much more appealing options for conducting precision measurements on Higgs physics. Three promising next-generation e^+e^- colliders, collectively referred to as Higgs factory: International Linear Collider (ILC) in Japan [4, 5], Future Circular Collider (FCC-ee) at CERN [6] (formerly called TLEP), and Circular Electron-Positron Collider (CEPC) in China [7, 8], have been proposed in recent years. All these three e^+e^- colliders plan to operate at center-of-mass (CM) energy around 250 GeV, where the dominant Higgs production channel is via the so-called Higgs-strahlung process, $e^+e^- \rightarrow HZ$. This golden process has been intensively studied theoretically in past several decades, *e.g.*, the leading order (LO) prediction was first given in Refs. [9, 10, 11], while the next-to-leading order (NLO) electroweak corrections were analyzed in Refs. [12, 13, 14]. Very recently, the mixed electroweak-QCD next-to-next-to-leading order (NNLO) corrections have also been investigated by two groups [15, 16], which yields the state-of-the-art prediction for $\sigma(HZ)$ about 230 fb around $\sqrt{s} = 240$ GeV.

The motif of this work is to study another type of Higgs production process at next-generation lepton colliders, the associated production of Higgs boson with a hard photon, that is, $e^+e^- \rightarrow H\gamma$. Owing to the exceedingly small electron-Higgs Yukawa coupling and absence of $H\gamma\gamma(Z)$ couplings at tree level, this process can only arise first at one-loop order in SM. The LO prediction to $\sigma(H\gamma)$ in SM is available long ago [17, 18, 19], which turns out to be several orders-of-magnitude smaller than that of $\sigma(HZ)$ around the Higgs factory energy.

Due to the highly suppressed cross section predicted in SM, the discovery of the $e^+e^- \rightarrow H\gamma$ process appears to be a rather unrealistic task in future e^+e^- colliders. Nevertheless, this may turn into a virtue, since this rare Higgs production process may serve a sensitive probe for new physics search. Had some new physics models induced notable modifications of the couplings between Higgs and gauge bosons/top quark, or had some hypothesized heavy charged particles strongly coupled to the Higgs boson, the $e^+e^- \rightarrow H\gamma$ process might even possibly be observed provided that $\sigma(H\gamma)$ were substantially enhanced relative to its SM value. The impact of possible new physics scenarios on this process have been extensively investigated in literatures [20, 21, 22, 23, 24, 25, 26].

Needless to say, an accurate SM prediction to $e^+e^- \rightarrow H\gamma$ is crucial and mandatory for confidently interpreting the potential new physics signal in future. The goal of this work is to carry out a comprehensive investigation on the NLO QCD corrections to this process in various energy range. In a sense, this two-loop calculation is similar to the previous works about NLO QCD corrections to $H \rightarrow \gamma\gamma$ [27, 28, 29, 30, 31, 32, 33, 34, 35, 36] and $H \rightarrow Z\gamma$ [37, 38, 39], whose magnitudes are found to be small. The situation in our case is more involved due to the occurrence of a new energy scale \sqrt{s} , and we are also interested in inferring how the effects of NLO QCD corrections vary with \sqrt{s} .

The rest of this paper is organized as follows. In section 2, we establish the notations and present theoretical descriptions of the NLO calculation. Section 3 is dedicated to presenting our numerical results and phenomenological discussions. We summarize in Section 4. For the convenience of the readers, the compact expressions for the LO amplitude are collected in Appendix.

2. Descriptions of the NLO calculation

Owing to the Lorentz covariance and electromagnetic current conservation, the amplitude for $e^+e^- \rightarrow H\gamma$ can be decomposed into the linear combination of four distinct Lorentz structures [19]:

$$\mathcal{M} = \sum_{i=1,2} C_i^\alpha \Lambda_i^\alpha, \quad (1)$$

where $C_{1,2}^\pm$ are scalar coefficients, and

$$\Lambda_1^\pm = \bar{v}(p_+)(1 \pm \gamma_5)(\not{\varepsilon}_\gamma p_\gamma \cdot p_- - \not{p}_\gamma \varepsilon_\gamma^* \cdot p_-)u(p_-), \quad (2a)$$

$$\Lambda_2^\pm = \bar{v}(p_+)(1 \pm \gamma_5)(\not{\varepsilon}_\gamma p_\gamma \cdot p_+ - \not{p}_\gamma \varepsilon_\gamma^* \cdot p_+)u(p_-), \quad (2b)$$

where p_+ and p_- signify the momenta of the incoming positron and electron, p_H and p_γ signify the momenta of the outgoing Higgs boson and photon, and ε_γ denotes the photon polarization vector. For simplicity, we will neglect the tiny electron mass throughout this work.

Substituting (2) into (1), squaring, and averaging upon initial-state e^\pm spins and summing over final-state photon helicity, we can express the differential cross section for $e^+e^- \rightarrow H\gamma$ as

$$\frac{d\sigma}{d\cos\theta} = \frac{1}{2s} \frac{s - m_H^2}{16\pi s} \frac{1}{4} \sum_{\text{pol}} |\mathcal{M}|^2 = \frac{s - m_H^2}{64\pi s} \left[t^2 (|C_1^+|^2 + |C_1^-|^2) + u^2 (|C_2^+|^2 + |C_2^-|^2) \right], \quad (3)$$

where θ denotes the polar angle between the the outgoing Higgs and the incoming positron, and m_H represents the Higgs boson mass. $s = (p_+ + p_-)^2$, $t = (p_H - p_+)^2$, and $u = (p_H - p_-)^2$ are standard Mandelstam variables.

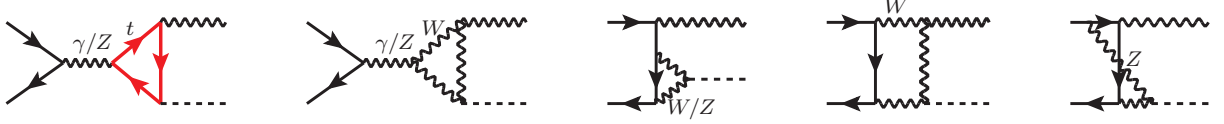


Figure 1: Representative LO Feynman diagrams for $e^+e^- \rightarrow H\gamma$ in SM.

This process first occurs at one-loop order in SM, with some representative diagrams shown in Fig. 1. The calculation of the LO amplitude has been comprehensively described in Refs. [17, 18, 19].

To assess the impact of the NLO QCD corrections, it is convenient to expand the form factors $C_{1,2}^\pm$ in powers of the strong coupling constant:

$$C_{1,2}^\pm = C_{1,2}^{\pm(0)} + \frac{\alpha_s}{\pi} C_{1,2}^{\pm(1)} + \dots, \quad (4)$$

where $C_{1,2}^{\pm(0)}$ signify the LO contributions, and $C_{1,2}^{\pm(1)}$ correspond to the $\mathcal{O}(\alpha_s)$ corrections.

Substituting (4) into (3), and employing $|C_{1,2}^\pm|^2 \approx |C_{1,2}^{\pm(0)}|^2 + 2\text{Re}[C_{1,2}^{\pm(0)} C_{1,2}^{\pm(1)*}]$, one then readily identifies the NLO QCD corrections to the cross section. The lowest-order expressions for $C_{1,2}^{\pm(0)}$ are well recorded in literatures [17, 18, 19]. The central challenge of this work is then to compute the four form factors $C_{1,2}^\pm$ through order α_s .

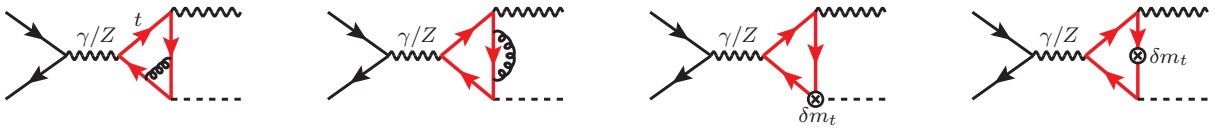


Figure 2: Typical Feynman diagrams for the NLO QCD corrections to $e^+e^- \rightarrow H\gamma$. The cap signifies the insertion of the top quark mass counterterm δm_t , as given in (7).

In our calculation, we employ Feynman gauge in both electroweak and QCD sectors. Moreover, we adopt the dimensional regularization to regularize both UV and IR divergences. The LO and NLO Feynman diagrams and corresponding amplitudes are generated by FeynArts [40]. We use the Mathematica packages FeynCalc/FeynCalcFormLink to carry out the trace over Dirac/color matrices [41, 42, 43], and utilize the packages Apart [44] (together with another self-written code) and the C++ code FIRE [45] to carry out partial fraction together with integration-by-parts (IBP) reduction for tensor integrals, and end up with a variety of master integrals (MIs).

For the LO amplitude, one needs include an electroweak counterterm for the $HZ\gamma$ coupling [46], in order to achieve UV-finite predictions. The corresponding $C_{1,2}^{\pm(0)}$ can then be expressed in terms of linear combinations of a number of one-loop Passarino-Veltman functions. In the previous works [17, 18, 19], these form factors have been presented in this format, yet assuming a non-vanishing electron mass to regulate the potential collinear divergence (which can arise from the last diagram in Fig. 1). Of course, the ultimate amplitude is free from collinear singularity and one is allowed to take the smooth limit $m_e \rightarrow 0$ in the end. As stated before, we have set $m_e = 0$ at the outset and instead used dimensional regularization to regularize both the UV and collinear divergences. We feel that our procedure is simpler both conceptually and technically. For the sake of completeness, and for readers' convenience, we present our compact expressions for $C_{1,2}^{\pm(0)}$ in the Appendix. These Passarino-Veltman functions can be numerically accurately computed by LoopTools [47] and Collier [48].

We wish to describe more details about the calculation of the NLO QCD corrections. At NLO, all the two-loop diagrams have simple s -channel topology, some of which are illustrated in Fig. 2. They can simply be obtained by dressing gluon to the top quark loop in the first LO diagram in Fig. 1. For simplicity, we have suppressed the contributions from the other 5 quark flavors due to their much smaller Yukawa couplings. Thanks to the simple s -channel topology, the amplitude assumes a factorized form:

$$\mathcal{M}^{(1)} = e\bar{v}(p_+)\gamma_\mu\left(g_e^-P_- + g_e^+P_+\right)u(p_-)\frac{1}{s-m_Z^2}\mathcal{T}_{ZH}^{\mu\nu}\varepsilon_{\gamma,\nu}^* + e\bar{v}(p_+)\gamma_\mu u(p_-)\frac{1}{s}\mathcal{T}_{\gamma H}^{\mu\nu}\varepsilon_{\gamma,\nu}^*, \quad (5)$$

where $P_\pm = \frac{1\pm\gamma_5}{2}$ are chirality projection operators. $g_f^- \equiv I_f^3/(s_W c_W) - Q_f s_W/c_W$, and $g_f^+ \equiv -Q_f s_W/c_W$, are the $Zf\bar{f}$ couplings for the left-handed and right-handed fermion f , respectively, where Q_f and I_f^3 correspond to the electric charge and the third component of the weak isospin of the fermion, and $c_W(s_W)$ stands for the cosine (sine) of the Weinberg angle. The two terms stem from the two-loop diagrams for $e^+e^- \rightarrow Z^* \rightarrow \gamma H$ and $e^+e^- \rightarrow \gamma^* \rightarrow \gamma H$, respectively, and $\mathcal{T}_{V\gamma H}^{\mu\nu}$ ($V = \gamma, Z$) represent the corresponding vertex form factors related to the $V\gamma H$ vertex.

At NLO, we only need consider the top quark loop contribution to the $V\gamma H$ vertex. Lorentz covariance and parity conservation enable us to parameterize the form factors $\mathcal{T}_{V\gamma H}^{\mu\nu}$ ($V = \gamma, Z$) as

$$\mathcal{T}_{V\gamma H}^{\mu\nu} = T_{V,1}p_\gamma^\mu p_\gamma^\nu + T_{V,2}k^\mu k^\nu + T_{V,3}p_\gamma^\mu k^\nu + T_{V,4}k^\mu p_\gamma^\nu + T_{V,5}p_\gamma \cdot k g^{\mu\nu}, \quad (6)$$

where $k = p_\gamma + p_H$ is the 4-momentum of the virtual gauge boson V , and $T_{V,i}$ ($i = 1, \dots, 5$) are various scalar form factors. Electromagnetic current conservation implies that $T_{V,2} = 0$, and $T_{V,3} = -T_{V,5}$. Furthermore, after substituting (6) into (5), one finds that $T_{V,1}$ and $T_{V,4}$ do not contribute to the amplitude. Consequently, we just need to calculate a single form factor $T_{V,5}$. We emphasize that, the mere QCD renormalization required in this work is to implement the top quark mass renormalization, with the mass counterterm:

$$\delta m_t = -\frac{3C_F}{4}\frac{\alpha_s}{\pi}\left[\frac{1}{\epsilon} + \frac{4}{3} + \ln\frac{4\pi\mu^2}{m_t^2} - \gamma_E\right]m_t, \quad (7)$$

where the spacetime dimension $d = 4 - 2\epsilon$, and m_t represents the top quark pole mass.

Having eliminated the UV divergence in $T_{V,5}$ that enters the NLO amplitude (5), after some straightforward algebras, one can identify the NLO coefficients $C_{1,2}^{\pm(1)}$ with

$$C_1^{\pm(1)} = C_2^{\pm(1)} = \frac{e}{2}g_e^\mp\frac{1}{s-m_Z^2}T_{Z,5} + \frac{e}{2s}T_{\gamma,5}. \quad (8)$$

Plugging this formula in (3), and with the aid of (4), we are able to deduce the intended NLO QCD corrections to the differential cross section.

We pause here to briefly describe our numerical strategy of computing the NLO corrections. After IBP reduction, we end up with about 38 two-loop MIs for $T_{V,5}$. We combine FIESTA [49]/CubPack [50] to perform the sector decomposition and the subsequent numerical integrations for MIs with quadruple precision. We also utilize the Fortran package Cuba [51] to crosscheck the numerical integrations for MIs.

It is worth mentioning that our two-loop calculation is analogous to the NLO QCD corrections calculation for $H \rightarrow Z\gamma$, which was recently accomplished by two groups in an analytic manner [38, 39]. As a crosscheck, we have

also revisited that process and found good agreement with the numerical results tabulated in [38]. Having passed such a nontrivial test, we feel confident about the correctness of our NLO QCD calculation for $e^+e^- \rightarrow H\gamma$.

By invoking crossing symmetry, our $T_{Z,5}$ can in principle be obtained from its counterpart in $H \rightarrow Z\gamma$ by performing some analytic continuation. Unfortunately, the analytic expressions recorded in Refs. [38, 39] involve rather lengthy and complicated special functions, rendering analytic continuation a non-trivial job. Therefore, we are content with presenting purely numerical, yet highly-accurate predictions in this letter.

3. Numerical results

In order to make concrete predictions, we specify the following input parameters in accordance with the latest compilation of Particle Data Group [52]:

$$\begin{aligned} M_W &= 80.385 \text{ GeV}, \quad M_Z = 91.1876 \text{ GeV}, \quad m_t = 174.2 \text{ GeV}, \\ m_H &= 125.09 \text{ GeV}, \quad \alpha = 1/137.035999139. \end{aligned} \quad (9)$$

In addition, the renormalization scale $\mu = \sqrt{s}$ is assumed for the running QCD coupling constant $\alpha_s(\mu)$. We choose to use the two-loop formula for α_s , which has been automated in the package RunDec [53].

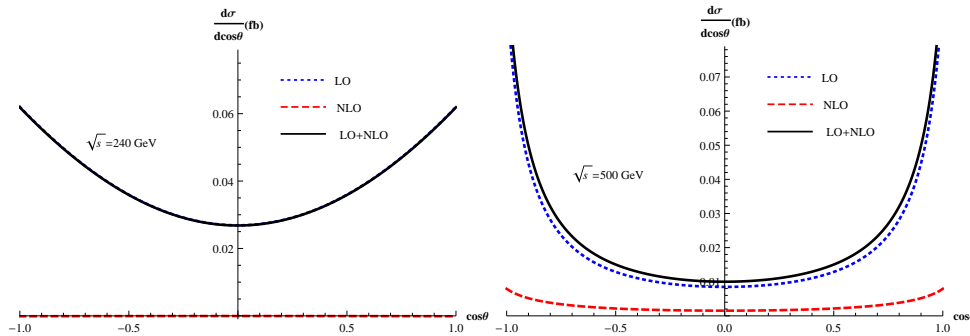


Figure 3: Differential cross sections for $e^+e^- \rightarrow H\gamma$ at $\sqrt{s} = 240$ GeV (left panel) and $\sqrt{s} = 500$ GeV (right panel).

In Fig. 3, we show the angular distribution of Higgs boson at two benchmark energy points, $\sqrt{s} = 240$ GeV at CEPC and 500 GeV at ILC, with both the LO and NLO predictions juxtaposed together. As can be clearly seen, the effect of NLO QCD corrections at CEPC is hardly discernible, but the impact of the NLO corrections becomes notable at the ILC energy.

To obtain the integrated cross section at each CM energy point, we utilize Cuba [51] to carry out the angular integration numerically. In Fig. 4, the dependence of the LO cross section on the CM energy is depicted over a wide range. There the line shape exhibits some interesting features. Starting from the threshold $\sqrt{s} = m_H$, the cross section rises due to the increment of the phase space. The cross section reaches its first peak around $\sqrt{s} = 250$ GeV, hits a dip around $\sqrt{s} = 400$ GeV, and then slowly bounces up and reaches the second flat peak at $\sqrt{s} = 500$ GeV. At asymptotic high energy, the cross section declines at a rate $\propto 1/s$, as expected from naive dimensional counting. To understand the origin of the peak-dip structure, we separate the contributions into two categories, those from the top quark loop and from the electroweak gauge bosons. From Fig. 4, one observes that there arises the severe destructive interference between these two channels, which should be responsible for this peculiar line-shape pattern.

In Fig. 5, we continue to show how the line shape of the integrated cross section varies with \sqrt{s} , including the NLO QCD correction. In most energy range, the impact of the NLO QCD corrections is rather mild, especially in $\sqrt{s} < 290$ GeV, with an relative correction typically less than 1%. Nevertheless, with the increasing CM energy, the corrections become more pronounced, and reaches the maximum around $\sqrt{s} \approx 400$ GeV. The effect of NLO corrections diminishes again as the CM energy further increases, completely negligible when $\sqrt{s} > 1$ TeV.

For concreteness and for clarity, in Table 1 we also enumerate the predicted cross sections in a wide range of CM energy, at both LO and NLO accuracy. In addition, we also tabulate the values of the scalar form factors $\tilde{T}_{\gamma/Z,5}$ at each

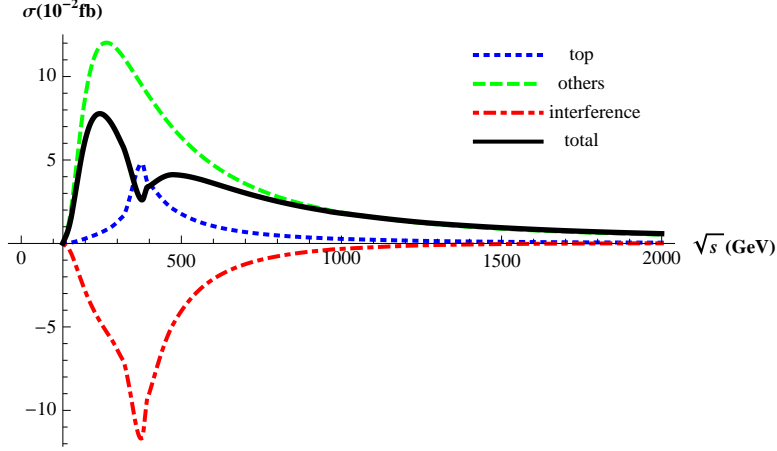


Figure 4: The LO cross section as a function of \sqrt{s} (The solid line). To trace the origin of the nontrivial line shape, we deliberately list the contributions from two classes of diagrams. The dotted, dashed and dot-dashed lines represent the contributions from the top quark loop, from all other diagrams that involve weak gauge bosons, and their interference, respectively.

$\sqrt{s}(\text{GeV})$	150	200	220	240	250	270	290	310	330
$\sigma^{\text{LO}} (10^{-2} \text{ fb})$	1.054	6.214	7.339	7.758	7.764	7.479	6.909	6.134	5.151
$\tilde{T}_{\gamma,5}(10^{-2}\text{GeV}^{-1})$	-0.793	-0.378	-0.112	0.251	0.485	1.12	2.11	3.90	8.16
$\tilde{T}_{Z,5}(10^{-2}\text{GeV}^{-1})$	0.290	0.138	0.041	-0.091	-0.177	-0.408	-0.772	-1.43	-2.98
$\sigma^{\text{NLO}}/\sigma^{\text{LO}}$	0.56%	0.30%	0.09%	-0.21%	-0.41%	-0.96%	-1.86%	-3.45%	-6.85%
$\sqrt{s}(\text{GeV})$	380	400	420	500	600	700	800	900	1000
$\sigma^{\text{LO}} (10^{-2} \text{ fb})$	2.977	3.433	3.763	4.079	3.604	3.018	2.518	2.118	1.801
$\tilde{T}_{\gamma,5} (10^{-2}\text{GeV}^{-1})$	-11.6 +16.6 <i>i</i>	-13.4 +9.81 <i>i</i>	-13.24 +5.76 <i>i</i>	-9.65 -1.29 <i>i</i>	-6.31 -3.21 <i>i</i>	-4.45 -3.48 <i>i</i>	-3.35 -3.38 <i>i</i>	-2.63 -3.19 <i>i</i>	-2.13 -3.00 <i>i</i>
$\tilde{T}_{Z,5}(10^{-2}\text{GeV}^{-1})$	4.25 -6.07 <i>i</i>	4.89 -3.65 <i>i</i>	4.84 -2.12 <i>i</i>	3.53 +0.471 <i>i</i>	2.31 +1.17 <i>i</i>	1.63 +1.27 <i>i</i>	1.22 +1.23 <i>i</i>	0.961 +1.17 <i>i</i>	0.779 +1.10 <i>i</i>
$\sigma^{\text{NLO}}/\sigma^{\text{LO}}$	16.81%	19.87%	19.24%	13.67%	9.60%	7.37%	5.98%	5.02%	4.31%

Table 1: The integrated cross sections of $e^+e^- \rightarrow H\gamma$ in a variety range of CM energy, at both LO and NLO accuracy. We also enumerate the corresponding values of the scalar form factors $T_{V,5}^{(1)}$ in (8). For simplicity, we have eliminated the α -dependence by invoking $\tilde{T}_{V,5}^{(1)} \equiv \alpha^{-3/2} T_{V,5}^{(1)}$.

energy. At CEPC energy range $\sqrt{s} \approx 250$ GeV, the QCD corrections have a really negligible effect; in contrast, if the ILC and FCC- ee could operate at $\sqrt{s} \approx 400$ GeV, the NLO corrections could reach about 20% of the LO prediction.

As can be noticed in Table 1, as $\sqrt{s} > 2m_t$, the form factors $T_{V,5}$ can develop an imaginary part, since the $t\bar{t}$ threshold opens up. It is worth mentioning that, when the CM energy gets very close to the 350 GeV, the fixed-order QCD perturbative expansion ceases to work, and an appropriate treatment would demand that a class of Coulomb gluon ladder diagrams must be resummed to all orders [54, 55, 56]. Such a treatment is beyond the scope of this work. Our NLO QCD predictions recorded in Table 1, still turn out to be reliable, where \sqrt{s} is always chosen to have some distance away from the $t\bar{t}$ threshold.

Finally, in Table 2 we further study the dependence of the NLO QCD corrections on the Higgs boson mass, with \sqrt{s} taken at the CEPC energy. The LO cross section decreases monotonously with the rising m_H , due to the shrinking phase space. The magnitudes of the NLO QCD corrections vary with m_H with a modest pace, nevertheless always less than 1%.

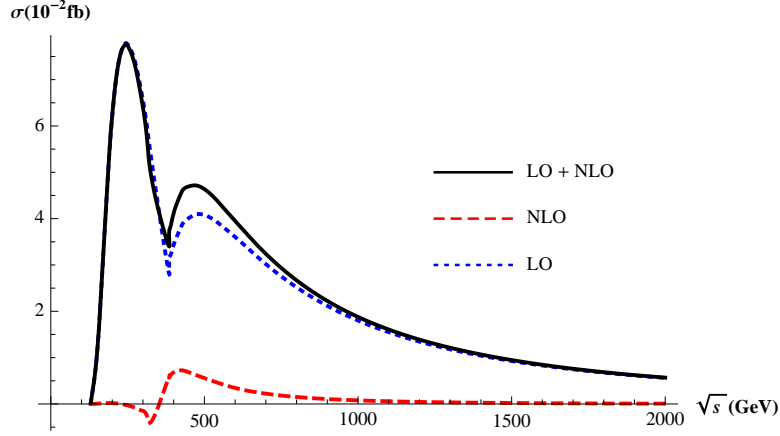


Figure 5: The integrated cross sections as a function of \sqrt{s} , both at LO and NLO.

$m_H(\text{GeV})$	40	60	80	100	120	140	160	180	200	220
$\sigma^{\text{LO}}(10^{-2} \text{ fb})$	15.46	14.15	12.43	10.42	8.293	6.288	5.454	3.212	1.170	0.1659
$\bar{T}_{\gamma,5}(10^{-4} \text{ GeV}^{-1})$	-3.70	0.101	5.59	12.9	22.3	34.2	48.9	67.1	89.7	118
$\bar{T}_{Z,5}(10^{-4} \text{ GeV}^{-1})$	1.35	-0.04	-2.04	-4.72	-8.46	-12.5	-17.9	-24.5	-32.8	-43.1
$\sigma^{\text{NLO}}(10^{-4} \text{ fb})$	0.524	-1.0×10^{-2}	-0.616	-1.16	-1.56	-1.70	-1.78	-1.27	-0.556	-9.6×10^{-2}

Table 2: Cross sections of $e^+e^- \rightarrow H\gamma$ as a function of Higgs boson mass, with \sqrt{s} fixed at 240 GeV.

4. Summary

The LO predictions for the production rate of $e^+e^- \rightarrow H\gamma$ in SM are rather small at the next-generation e^+e^- colliders, which renders it an attractive channel to search for the elusive footprint of the beyond-SM physics. An accurate SM prediction to this process is compulsory for confronting the potential new physics signal in the future. In this letter, we have, for the first time, calculated the NLO QCD corrections to this associated $H + \gamma$ production process, and conducted a comprehensive numerical study covering a wide range of CM energy. The key finding is that, the NLO QCD corrections to this process at CEPC are completely negligible, but may have sizable effect at ILC.

Appendix: The analytic expressions for $C_{1,2}^{\pm(0)}$

For reader's convenience, here we list the compact expressions for the LO coefficients functions $C_{1,2}^{\pm(0)}$ appearing in (3), with m_e set to zero in the outset. They can be split into three parts:

$$C_i^{\pm(0)} = a^2 \left[\sum_{V=Z,\gamma} \frac{g_{V_e}^{\mp} m_W}{2s_W(s - m_V^2)} C_{Vi}^{\pm(0,\text{vert})} - \frac{m_W}{s_W^3} C_i^{\pm(0,\text{Wbox})} + \frac{2m_W}{s_W c_W^2} C_i^{\pm(0,\text{Zbox})} \right], \quad (10)$$

where $i = 1, 2$, and

$$\begin{aligned}
C_{Vi}^{\pm(0,\text{vert})} &= \frac{4}{3} \frac{m_t^2}{m_W^2} N_c (g_{Vt}^- + g_{Vt}^+) (C_0^a + 4C_2^a + 4C_{12}^a + 4C_{22}^a) \\
&+ 4 \frac{m_H^2}{m_W^2} c_{V2} (C_2^b + C_{12}^b + C_{22}^b) + c_{V1} (10C_0^b - 2C_1^b + 17C_2^b + 19C_{12}^b + 19C_{22}^b) \\
&+ 2c_{V2} (2C_0^b + 2C_1^b + 3C_2^b + C_{12}^b + C_{22}^b) + c_{V3} (2C_0^b - 2C_1^b + C_2^b + 3C_{12}^b + 3C_{22}^b), \tag{11a}
\end{aligned}$$

$$C_1^{+(0,\text{Wbox})} = D_1^a + D_1^b + D_{13}^b - D_{13}^a - D_{33}^a, \tag{11b}$$

$$C_2^{+(0,\text{Wbox})} = D_2^a + D_{23}^a + D_2^b - D_{23}^b - D_{33}^b, \tag{11c}$$

$$C_{1,2}^{-(0,\text{Wbox})} = 0, \tag{11d}$$

$$C_1^{\pm(0,\text{Zbox})} = g_e^\mp (D_2^c + D_{12}^c + D_{23}^c), \tag{11e}$$

$$C_2^{\pm(0,\text{Zbox})} = g_e^\mp (D_{13}^c + D_{33}^c), \tag{11f}$$

where $g_{Zf}^\pm = g_f^\pm$, $g_{\gamma f}^\pm = -Q_f$, and we define $c_{Z1} \equiv -c_W/s_W$, $c_{Z2} \equiv (s_W^2 - c_W^2)/(2s_W c_W)$, $c_{Z3} \equiv s_W/c_W$, $c_{\gamma 1} = c_{\gamma 2} = c_{\gamma 3} \equiv 1$, and

$$C_{ij\dots}^a \equiv C_{ij\dots}(0, s, m_H^2, m_t^2, m_t^2, m_t^2), \tag{12a}$$

$$C_{ij\dots}^b \equiv C_{ij\dots}(0, s, m_H^2, m_W^2, m_W^2, m_W^2), \tag{12b}$$

$$D_{ij\dots}^a \equiv D_{ij\dots}(0, s, m_H^2, u, 0, 0, 0, m_W^2, m_W^2, m_W^2), \tag{12c}$$

$$D_{ij\dots}^b \equiv D_{ij\dots}(0, s, 0, t, 0, m_H^2, 0, m_W^2, m_W^2, m_W^2), \tag{12d}$$

$$D_{ij\dots}^c \equiv D_{ij\dots}(0, u, m_H^2, t, 0, 0, 0, 0, m_Z^2, m_Z^2). \tag{12e}$$

We use the same conventions for the Passarino-Veltman scalar functions as in most modern literatures (see, for instance, Ref. [48]). Note that the functions (12e), which are affiliated with the last diagram in Fig. 1, are by themselves free from any collinear singularity. If the IBP reduction is further implemented for (12e), one will end up with a linear combination of a handful of one-loop MIs, some of which are IR divergent. Fortunately, one can use LoopTools [47] and Collier [48] to directly calculate these Passarino-Veltman functions in (12).

Acknowledgments

W.-L. S. is supported by the National Natural Science Foundation of China under Grants No. 11447031 and No. 11605144, by the Natural Science Foundation of ChongQing under Grant No. cstc2014jcyjA00029, and also by the Fundamental Research Funds for the Central Universities under Grant No. XDJK2016C067. The work of W. C. and Y. J. is supported in part by the National Natural Science Foundation of China under Grants No. 11475188, No. 11261130311, No. 11621131001 (CRC110 by DGF and NSFC), by the IHEP Innovation Grant under contract number Y4545170Y2, and by the State Key Lab for Electronics and Particle Detectors. The work of F. F. is supported by the National Natural Science Foundation of China under Grant No. 11505285, and by the Fundamental Research Funds for the Central Universities. Q.-F. S. is supported by the National Natural Science Foundation of China under Grant No. 11375168 and No. 11475188. The Feynman diagrams in this paper were prepared using JaxoDraw [57, 58].

References

- [1] G. Aad *et al.* [ATLAS Collaboration], Phys. Lett. B **716** (2012) 1 doi:10.1016/j.physletb.2012.08.020 [arXiv:1207.7214 [hep-ex]].
- [2] S. Chatrchyan *et al.* [CMS Collaboration], Phys. Lett. B **716** (2012) 30 doi:10.1016/j.physletb.2012.08.021 [arXiv:1207.7235 [hep-ex]].
- [3] G. Aad *et al.* [ATLAS and CMS Collaborations], JHEP **1608** (2016) 045 doi:10.1007/JHEP08(2016)045 [arXiv:1606.02266 [hep-ex]].
- [4] H. Baer *et al.*, arXiv:1306.6352 [hep-ph].
- [5] D. M. Asner *et al.*, arXiv:1310.0763 [hep-ph].

- [6] M. Bicer *et al.* [TLEP Design Study Working Group Collaboration], JHEP **1401**, 164 (2014) [arXiv:1308.6176 [hep-ex]], <http://tlep.web.cern.ch/>
- [7] CEPC-SPPC Study Group, IHEP-CEPC-DR-2015-01, IHEP-TH-2015-01, HEP-EP-2015-01.
- [8] CEPC-SPPC Study Group, IHEP-CEPC-DR-2015-01, IHEP-AC-2015-01.
- [9] J. R. Ellis, M. K. Gaillard and D. V. Nanopoulos, Nucl. Phys. B **106**, 292 (1976).
- [10] B. L. Ioffe and V. A. Khoze, Sov. J. Part. Nucl. **9**, 50 (1978) [Fiz. Elem. Chast. Atom. Yadra **9**, 118 (1978)].
- [11] J. D. Bjorken, Conf. Proc. C **7608021**, 1 (1976).
- [12] J. Fleischer and F. Jegerlehner, Nucl. Phys. B **216** (1983) 469.
- [13] B. A. Kniehl, Z. Phys. C **55** (1992) 605.
- [14] A. Denner, J. Kublbeck, R. Mertig and M. Bohm, Z. Phys. C **56** (1992) 261.
- [15] Q. F. Sun, F. Feng, Y. Jia and W. L. Sang, arXiv:1609.03995 [hep-ph].
- [16] Y. Gong, Z. Li, X. Xu, L. L. Yang and X. Zhao, arXiv:1609.03955 [hep-ph].
- [17] A. Barroso, J. Pulido and J. C. Romao, Nucl. Phys. B **267** (1986) 509. doi:10.1016/0550-3213(86)90128-8
- [18] A. Abbasabadi, D. Bowser-Chao, D. A. Dicus and W. W. Repko, Phys. Rev. D **52** (1995) 3919 doi:10.1103/PhysRevD.52.3919 [hep-ph/9507463].
- [19] A. Djouadi, V. Driesen, W. Hollik and J. Rosiek, Nucl. Phys. B **491** (1997) 68 doi:10.1016/S0550-3213(96)00711-0 [hep-ph/9609420].
- [20] G. J. Gounaris, F. M. Renard and N. D. Vlachos, Nucl. Phys. B **459** (1996) 51 doi:10.1016/0550-3213(95)00602-8 [hep-ph/9509316].
- [21] U. Mahanta, Phys. Lett. B **423** (1998) 126. doi:10.1016/S0370-2693(98)00113-0
- [22] A. Arhrib, R. Benbrik and T. C. Yuan, Eur. Phys. J. C **74** (2014) 2892 doi:10.1140/epjc/s10052-014-2892-5 [arXiv:1401.6698 [hep-ph]].
- [23] S. L. Hu, N. Liu, J. Ren and L. Wu, J. Phys. G **41** (2014) no.12, 125004 doi:10.1088/0954-3899/41/12/125004 [arXiv:1402.3050 [hep-ph]].
- [24] H. Y. Ren, Chin. Phys. C **39** (2015) no.11, 113101 doi:10.1088/1674-1137/39/11/113101 [arXiv:1503.08307 [hep-ph]].
- [25] Q. H. Cao, H. R. Wang and Y. Zhang, Chin. Phys. C **39** (2015) no.11, 113102 doi:10.1088/1674-1137/39/11/113102 [arXiv:1505.00654 [hep-ph]].
- [26] G. Li, H. R. Wang and S. h. Zhu, Phys. Rev. D **93** (2016) no.5, 055038 doi:10.1103/PhysRevD.93.055038 [arXiv:1506.06453 [hep-ph]].
- [27] H. Q. Zheng and D. D. Wu, Phys. Rev. D **42** (1990) 3760. doi:10.1103/PhysRevD.42.3760
- [28] A. Djouadi, M. Spira, J. J. van der Bij and P. M. Zerwas, Phys. Lett. B **257** (1991) 187. doi:10.1016/0370-2693(91)90879-U
- [29] S. Dawson and R. P. Kauffman, Phys. Rev. D **47** (1993) 1264. doi:10.1103/PhysRevD.47.1264
- [30] A. Djouadi, M. Spira and P. M. Zerwas, Phys. Lett. B **311** (1993) 255 doi:10.1016/0370-2693(93)90564-X [hep-ph/9305335].
- [31] K. Melnikov and O. I. Yakovlev, Phys. Lett. B **312** (1993) 179 doi:10.1016/0370-2693(93)90507-E [hep-ph/9302281].
- [32] M. Inoue, R. Najima, T. Oka and J. Saito, Mod. Phys. Lett. A **9** (1994) 1189. doi:10.1142/S0217732394001003
- [33] M. Spira, A. Djouadi, D. Graudenz and P. M. Zerwas, Nucl. Phys. B **453** (1995) 17 doi:10.1016/0550-3213(95)00379-7 [hep-ph/9504378].
- [34] J. Fleischer, O. V. Tarasov and V. O. Tarasov, Phys. Lett. B **584** (2004) 294 doi:10.1016/j.physletb.2004.01.063 [hep-ph/0401090].
- [35] R. Harlander and P. Kant, JHEP **0512** (2005) 015 doi:10.1088/1126-6708/2005/12/015 [hep-ph/0509189].
- [36] U. Aglietti, R. Bonciani, G. Degrossi and A. Vicini, JHEP **0701** (2007) 021 doi:10.1088/1126-6708/2007/01/021 [hep-ph/0611266].
- [37] M. Spira, A. Djouadi and P. M. Zerwas, Phys. Lett. B **276** (1992) 350. doi:10.1016/0370-2693(92)90331-W
- [38] R. Bonciani, V. Del Duca, H. Frellesvig, J. M. Henn, F. Moriello and V. A. Smirnov, JHEP **1508** (2015) 108 doi:10.1007/JHEP08(2015)108 [arXiv:1505.00567 [hep-ph]].
- [39] T. Gehrmann, S. Guns and D. Kara, JHEP **1509**, 038 (2015) [arXiv:1505.00561 [hep-ph]].
- [40] T. Hahn, Comput. Phys. Commun. **140**, 418 (2001) [hep-ph/0012260].
- [41] R. Mertig, M. Bohm and A. Denner, Comput. Phys. Commun. **64**, 345 (1991).
- [42] V. Shtabovenko, R. Mertig and F. Orellana, Comput. Phys. Commun. **207** (2016) 432 doi:10.1016/j.cpc.2016.06.008 [arXiv:1601.01167 [hep-ph]].
- [43] F. Feng and R. Mertig, arXiv:1212.3522.
- [44] F. Feng, Comput. Phys. Commun. **183**, 2158 (2012) [arXiv:1204.2314 [hep-ph]].
- [45] A. V. Smirnov, Comput. Phys. Commun. **189**, 182 (2014) [arXiv:1408.2372 [hep-ph]].
- [46] A. Denner, Fortsch. Phys. **41**, 307 (1993) [arXiv:0709.1075 [hep-ph]].
- [47] T. Hahn and M. Perez-Victoria, Comput. Phys. Commun. **118**, 153 (1999) [hep-ph/9807565].
- [48] A. Denner, S. Dittmaier and L. Hofer, Comput. Phys. Commun. **212** (2017) 220 doi:10.1016/j.cpc.2016.10.013 [arXiv:1604.06792 [hep-ph]].
- [49] A. V. Smirnov, Comput. Phys. Commun. **204** (2016) 189 doi:10.1016/j.cpc.2016.03.013 [arXiv:1511.03614 [hep-ph]].
- [50] R. Cools and A. Haegemans, ACM Trans. Math. Softw. **29** (2003), no. 3 287 C296.
- [51] T. Hahn, Comput. Phys. Commun. **168** (2005) 78 doi:10.1016/j.cpc.2005.01.010 [hep-ph/0404043].
- [52] C. Patrignani *et al.* [Particle Data Group], Chin. Phys. C **40** (2016) no.10, 100001. doi:10.1088/1674-1137/40/10/100001
- [53] K. G. Chetyrkin, J. H. Kuhn and M. Steinhauser, Comput. Phys. Commun. **133**, 43 (2000) [hep-ph/0004189].
- [54] V. S. Fadin and V. A. Khoze, JETP Lett. **46** (1987) 525 [Pisma Zh. Eksp. Teor. Fiz. **46** (1987) 417].
- [55] V. S. Fadin and V. A. Khoze, Sov. J. Nucl. Phys. **48** (1988) 309 [Yad. Fiz. **48** (1988) 487].
- [56] M. J. Strassler and M. E. Peskin, Phys. Rev. D **43** (1991) 1500. doi:10.1103/PhysRevD.43.1500
- [57] D. Binosi and L. Theussl, Comput. Phys. Commun. **161**, 76 (2004) doi:10.1016/j.cpc.2004.05.001 [hep-ph/0309015].
- [58] D. Binosi, J. Collins, C. Kaufhold and L. Theussl, Comput. Phys. Commun. **180** (2009) 1709 doi:10.1016/j.cpc.2009.02.020 [arXiv:0811.4113 [hep-ph]].